Transporting MIL-STD-1553 Signals by Means of Optical Wireless Interfaces

G. Cossu, L. Gilli, E. Ertunc, and E. Ciaramella, *Senior Member, IEEE*

***Abstract*—Today, the on-board Spacecraft (SC) communication requires an impressive network of massive wires, both in flight and in the Assembly Integration and Test (AIT) phase. Here, we present the design and the experimental characterization of novel Optical Wireless Communication (OWC) transceivers compatible with MIL-STD-1553B, which is the shared bus predominantly deployed in SCs. Each transceiver works as an interface that transports the bipolar Manchester-coded signal by converting it to/from the optical domain. These OWC interfaces can effectively reduce the overall weight and cost of the SC and can also largely decrease the AIT time. Since they are fully analog and do not need any microprocessors or Digital Signal Processing, they have a small footprint and a very low power consumption. We initially characterize the transceivers using a non-return-to-zero (NRZ) signal, then we used them to replace a cable and connect a pair of test units, transmitting MIL-STD-1553B signals: the measurements show that our solution has a good power budget (+65dB), which will allow the interoperability with MIL-STD-1553B boards in a wide range of scenarios. Furthermore, it is realized by means of commercially available components; it could also be implemented by using proven space-graded devices.**

***Index Terms*—Wireless communication, light emitting diode, vertical cavity surface-emitting.**

I. Introduction

VARIOUS types of data bus are used today on SCs for the intensive on-board communication among sensors and pieces of equipment [1]. Among them, MIL-STD-1553B is one of the most widely used [2], thanks to its proven robustness [3].

All avionics buses are supported by huge amounts of wires so that around 8% of the total dry mass of a SC is due to the cables and electrical interfaces [4]. Comparable figures and issues are also reported about wired networks on aircrafts, where similar solutions are deployed. Furthermore, wired networks have other drawbacks: they require time and cost for routing, placing, and shielding the cables [5], [6]. There is clearly a high potential in replacing these wires by moving to wireless communications [7]–[9]. Yet this is far to be achieved, although the benefits in terms of costs would be remarkable [10].

Initially, wireless communications based on Radio Frequency (RF) had been considered [9], [11], but it was soon apparent that they could not be used on SC because of Electro-Magnetic Interference (EMI) on the electrical equipment. Moreover, in order to avoid crosstalk effects, arrays of antennas could be required to produce directional beams [12], [13].

As an alternative, OWC solutions had been proposed [14]; OWC systems are based on modulated optical signals, either in the visible or in the Infrared (IR) region, and usually exploit intensity modulation at the transmitter and direct detection at the receiver by a Photo-Diode (PD). This option for the MIL-STD-1553B bus on a SC was initially investigated 20 years ago [15]–[18]. However, it was found that the specific features of the MIL-STD-1553B bus make it unsuitable for a straight adaptation to OWC [19]. Therefore, Serial Peripheral Interface (SPI) and ad-hoc developed protocols were introduced in order to prove the feasibility [17]. In addition, the solution had also to include Wavelength Division Multiplexing (WDM), Frequency Division Multiplexing (FDM) and Time Division Multiplexing (TDM), plus a range of modulation formats (Manchester, On-Off Keying, etc.) and, in some cases, even Digital Signal Processing (DSP). Although the final tests were positive, the realized prototypes were too complex, bulky and heavy for the satellite requirements [17], [20] and were thus not considered for further studies.

Later on, OWC systems explicitly based on Field Programmable Gate Array (FPGA) were proposed [21], [22]. Their transmission performance was either not reported [21], or very poor (the packet error rate was 13% [22]). Moreover, because of DSP, they suffered from high complexity, latency, and power consumption.

Recent developments in OWCs [23] renewed the interest in wireless solutions based on optical carriers [24]. As a noteworthy fact, today, OWCs systems can take advantage of new Commercial Off-the-Shelf (COTS) components at the Transmitter (TX) and at the Receiver (RX). These devices allow the design of OWC systems that are application-specific, e.g. they can be precisely tailored for low (high) bit-rates covering a wide (small) area: the lower is the bit rate, the higher is the robustness of the optical link [24]–[27]. In the particular case of MIL-STD-1553B, the signal bit rate is very moderate: this results into relaxed constrains in terms of minimum optical power intensity at the RX. Therefore, it is possible to use a TX with a very diverging beam and even exploit reflections from the walls: these features make it suitable for deployment even on for intra-SC communications, where line-of-sight can be unfeasible and many shadowing objects will be present.

In this framework, European Space Agency (ESA) endorsed the project Transmission of Optical Wireless Signals for telecom

Manuscript received August 5, 2021; revised December 6, 2021; accepted December 24, 2021. Date of publication December 28, 2021; date of current version January 6, 2022. This work was supported by ESA Project TOWS under Contract 4000125458/18/U.K./NR. *(Corresponding author: Giulio Cossu.)*

The authors are with the Istituto di Tecnologie della Comunicazione, dell'Informazione e della Percezione, Scuola Superiore Sant'Anna, 56124 Pisa, Italy (e-mail: ernesto.ciaramella@sssup.it; g.cossu@santannapisa.it; e.ertunc@santannapisa.it; l.gilli@santannapisa.it).

Digital Object Identifier 10.1109/JPHOT.2021.3138973

satellites (TOWS) that should develop novel and simple interfaces for MIL-STD-1553B bus to be transported over OWC so that they can be considered for practical deployment. To this aim, TOWS is proposing a distinctive approach by exclusively working at the physical layer [28]. Thus the cabled connections of the whole MIL-STD-1553B bus would be replaced seamlessly by wireless transmission without any other modification to the equipment. This is a completely different target, as TOWS is realizing transparent OWC links able to replace today wires in all the considered application scenarios. As a key feature, the proposed transceivers will be fully analog and will work as a physical interface, maintaining the compatibility with the existing hardware, requiring no modification of the protocol and of the bus architecture: this is a key issue to keep the costs low, avoiding the need for smart devices, such as FPGAs or processors. In order to have practical relevance, the solution should have also other practical features: it should have minimal footprint, have low weight, and have low power consumption [28].

TOWS will address three application scenarios, each having specific functional requirements, i.e. intra-SC, extra-SC and AIT. Therefore, the developed hardware should implement a flexible architecture that can be easily tuned to the different application scenarios with only minor modifications of the hardware [28].

Here, we present for the first time the design and the experimental characterization of these novel transparent OWC-1553 interfaces: they prove that wireless transmission of MIL-STD-1553B signals is feasible and this result is achieved by transceivers that are realized by using commercially common components, and have limited size and low weight. First, in Section II, we briefly summarize the most relevant features of the MIL-STD-1553B standard and discuss the issues of adapting to OWC. In Section III, we introduce our novel design of the boards that should allow the seamless interoperability between MIL-STD-1553B units and OWC. In Section IV we present and discuss the experimental characterization of the novel OWC systems, first as stand-alone and then interfaced with MIL-STD-1553B test equipment and we prove their interoperability with MIL-STD-1553B boards. Finally, in Section V, we summarize the key results and draw the conclusion.

II. MIL-STD-1553 Standard

The MIL-STD-1553B standard defines a digital time division command/response multiplexed data bus [19], which is a terminated transmission line based on a twisted and shielded pair of wires; it has a 1Mbit/s fixed data rate and is typically implemented as a dual standby redundant architecture [19].

The MIL-STD-1553B uses Manchester II bi-phase bit encoding. A typical sequence is shown in Fig. 1(a). A logic 1 is transmitted as a positive amplitude (high state, H) followed by a negative pulse (low state, L), this is reversed for a logic 0. The idle state is encoded with amplitude 0 V. The peak-to-peak output voltage of the transmitter is 18 to 27 V [19].

As the bit rate is equal to 1 Mbit/s, the bit time is equal to 1 μs, with a voltage transition at the midpoint. The MIL-STD-1553B

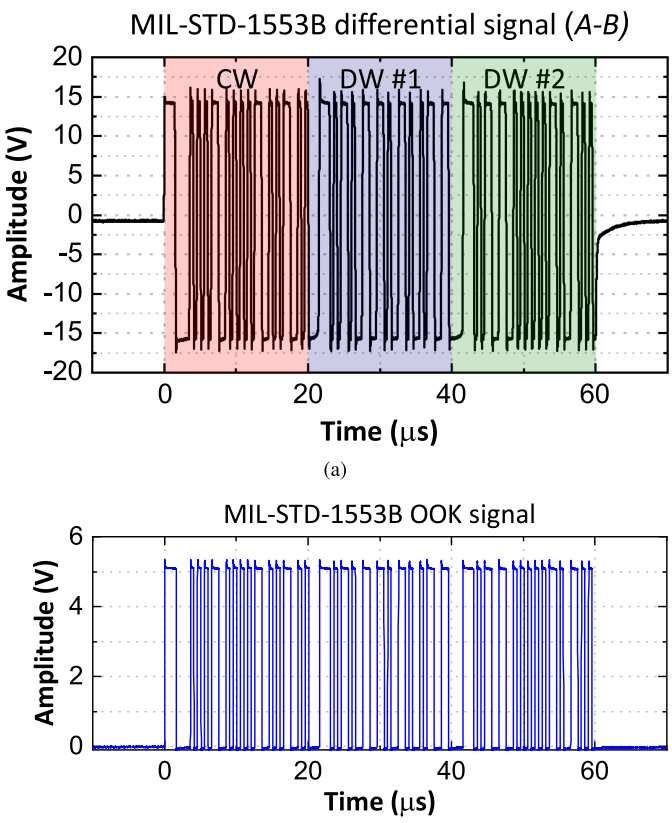

Fig. 1. Typical MIL-STD-1553B signal with one Command Word and two Data Words (a) and corresponding single-ended OOK output from the signal adaptation (b).

signal is sent by a transceiver over a shared bus, which is made of a pair of wires, as a differential voltage. A third wire is the ground, for a total of three electrical lines. The bus conveys data packets, named *words*. Each word includes a synchronization sequence with a time window of 3 μs, a 16 bit long sequence and an additional parity bit, for a total of 20 μs. As an example, in Fig. 1(a), we report a MIL-STD-1553B waveform composed by 1 Command Word (CW) and 2 Data Words (DWs). In the OWC implementation we should transmit unipolar signals. Moreover, to reduce the power consumption, we choose to bias the signal so that when the bus is not active all the light sources are turned off. Fig. 1(b) shows the corresponding unipolar signal that we transmit over OWC.

Three types of devices can transmit data on the shared bus: Bus Controller (BC), Remote Terminal (RT) and Bus Monitor (BM). Although these devices have different tasks, our OWC transceivers will be the same in each specific scenario: the key point is that they are designed to work only at the Physical Layer, to replace the cables. Thus, the rest of the network is not affected, neither is sensitive to the replacement. To achieve this goal, clearly, the transceivers must be carefully designed so that they perfectly work with the MIL-STD-1553B interfaces and the whole electronics at that level behaves exactly as if a physical cable were present.

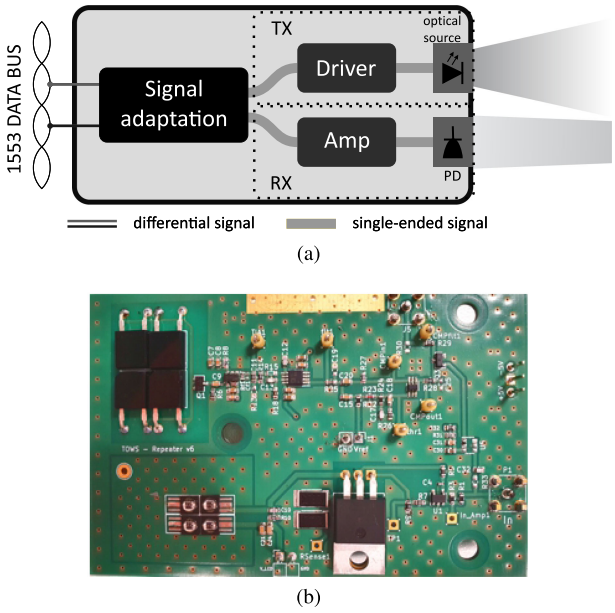

Fig. 2. Transceiver building blocks (a) and picture of the realized board (b).

III. Design of the Optical Wireless Solution

In this section, we present the design of the TOWS transceivers and discuss their key elements.

Each transceiver board is composed of three functional parts: the signal adaptation, the TX and the RX. This is illustrated in Fig. 2, which also reports a picture of one board. As can be seen, the board has a limited size, which can be strongly reduced by further optimization. The current electrical power consumption is around $600\,\mathrm{mW}$, which is considered a perfectly acceptable value.

The adaptation electronics consists of a Printed Circuit Board (PCB) with a MIL-STD-1553B input/output interface and the electronics to adapt the electric signal levels to/from the optical devices. It is the same in the three implementations: it converts the MIL-STD-1553B bipolar differential signal to a unipolar On-Off Keying (OOK) format, compatible with TX and, viceversa, it converts the OOK format from the RX to a MIL-STD-1553B signal (see Fig. 1(a) and Fig. 1(b)).

We recall that the transceivers for the BC and the RTs are the exactly same, whilst the BM needs no TX.

The redundancy and error handling are also fully inherited from the MIL-STD-1553B protocol. In particular, as far as the redundancy is concerned, each connector (main and redundant) on the terminal shall be interfaced with an OWC transceiver to maintain the standard bus redundancy. There will be no crosstalk between the two parallel buses, since they operate alternatively.

The transmitter and receiver can host slightly different opto-electronic devices depending on the specific application scenario. The different application scenarios require to develop systems working in different transmission configurations. These link configurations belong to two different categories: Non Line-of-Sight (NLOS) or Directed Line-of-Sight (DLOS). In a DLOS configuration, we have an optical transmission with a direct line of sight between TX and RX. In this configuration, a narrow light beam is used and the required transmitted power is low. On the other hand, in the NLOS configuration, an optical link is established without a direct line of sight between TX and RX, as it indeed exploits reflections. Clearly, NLOS configurations need higher transmitted optical power, wider emission angle at TX and wider Field-of-View (FOV) at RX.

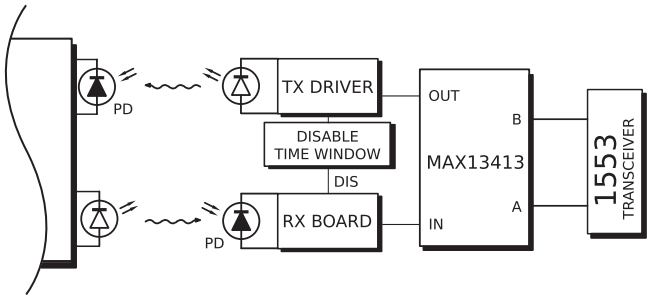

Fig. 3. Schematics of the signal adapter from the MIL-STD-1553B transceiver to the optical TX and RX, including the disable time window.

Regarding TOWS scenarios, transmitter and receiver will work in a NLOS architecture for intra-SC and AIT scenarios, whilst they could use DLOS in the extra-SC communications [28]. According to these configuration differences, TX and RX will exploit different optoelectronic devices. In the following sections, we describe the implementation of the proposed transceiver, illustrating its three units.

A. Signal Adaptation

As anticipated, the native MIL-STD-1553B signal has many features that make it hard to be transported by a OWC link. Indeed, a MIL-STD-1553B waveform is a differential bipolar signal that exploits the same three electrical lines (positive, negative and ground signals) for both link directions over the shared bus. Hence, the information cannot be directly transmitted/received over an OWC system, which is made of two independent unidirectional links.

In order to overcome the above issues, we developed an original signal adapter that recognizes the direction of the data flow without the need of a custom DSP. Therefore, depending on the transmission mode, the adapter correctly conveys the signals on TX or RX section of the OWC part. To this aim, we start from a chip by Maxim, which includes an automatic flow controller and was originally designed for the RS485/RS422 standards. These standards are quite similar to the MIL-STD-1553B, so that an adaptation is feasible, although not straightforward.

The scheme of the signal adapter is presented in Fig. 3. The chip (MAX13413) has two input/output ports, *A* and *B*, which are able to transmit/receive a differential bipolar signal, and two independent output and input ports (see Fig. 3), which generate (*OUT*) or receive (*IN*) the corresponding single-ended OOK signal. The chip can work in two different modes: TX-mode and RX-mode. In the TX-mode, *A* and *B* ports work as inputs to the chip; the *OUT* port is enabled to transmit the signal to the OWC driver. In RX-mode, *A* and *B* ports work as output from

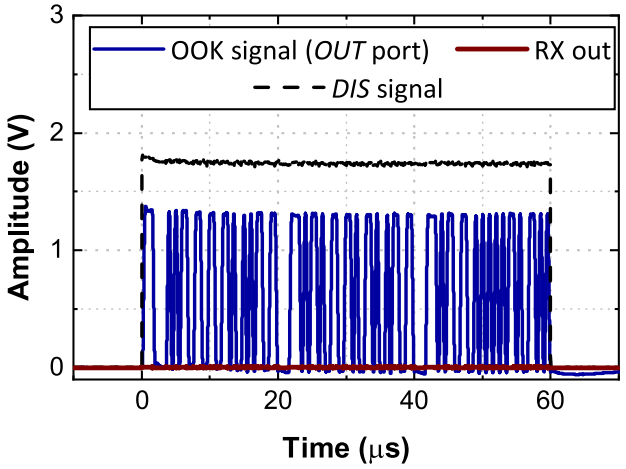

Fig. 4. Electrical suppression of the cross-talk due to back reflections: we report the signal detected by the PD (TIA output) in blue line, the generated disable time window in black, and the receiver output in red.

the chip. In our case, the *IN* port is enabled to receive the OWC signal and the *OUT* port is disabled to avoid cross-talk with the TX section. In addition to the conversion from differential to single-ended, the chip performs also a voltage adaptation from/to the *A*-*B* signal ($-15\,\mathrm{V}$ to $+15\,\mathrm{V}$ as in Fig. 1(a)) to/from the OOK signal of the *IN* and *OUT* ports ($0\,\mathrm{V}$ to $5\,\mathrm{V}$ as in Fig. 1(b)). This voltage conversion allows to switch off the optical source when no data is transmitted (the idle state corresponds to $0\,\mathrm{V}$), reducing the overall power consumption of the proposed OWC transceiver.

We highlight that, using only the chip, any reflection can produce a cross-talk between the RX and TX on the same transceiver, because *IN* is not disabled in TX-mode [29]. To solve this issue, we spill a part of the signal to the TX and use it to generate a disable signal (*DIS* in Fig. 4). This last is used to disable the RX board circuitry, thus suppressing the effect of the optical reflections.

In summary, two types of cross talk could occur during the bidirectional transmission. In RX-mode, we can have an electrical cross talk on the signal adaptation operation. As mentioned before, the A and B port of the chip work as both input and output, which means that they are connected to the same electrical node as IN and OUT ports. When a signal is received through the IN port, this could be transmitted by the OUT port causing the cross talk. Nevertheless, the chip itself disables the OUT port in RX-mode avoiding this effect. In TX-mode different types of cross talk can be produced, optical cross talk could occur if the RX detects back reflections of the signal from the TX of the same transceiver. In order to avoid this effect, the RX board circuitry is temporarily disabled within a rectangular pulse during the transmission (*DIS* in Fig. 4).

In order to demonstrate its operation, we realized a setup where we emulated a maximized optical cross-talk: the TX and RX of the same transceiver were separated and placed one in front of the other. In Fig. 4, we report the TX signal (blue line), the *DIS* time window (black dashed line) and RX signal output (red line) as it turns out with the RX circuitry disabled. As can be seen, the disable window effectively works and suppresses the RX signal: as a result, we obtain a very weak ($<10\,\mathrm{mV}$) electrical cross-talk that enters in *IN*. This is negligible: as it is much lower than the internal threshold ($200\,\mathrm{mV}$) of the MAX13413, thus it is clipped by the chip itself.

B. Transmitter

In TOWS approach, the transparent OWC transceivers will be used in the three different scenarios with a modular scheme, where the same key elements are always used and few minor changes are enough to optimize the solution in each scenario [28]. This affects the design of both TX and RX. First, in the intra-SC environment we have no background light, but the light-wave signals suffer from severe shadowing effects; in that case, TOWS should implement a NLOS architecture, where OWC exploits the reflections from the walls/ceiling [30]. Similarly, in the AIT scenario, shadowing will make preferable a NLOS architecture, exploiting the (strong) scattering from the ceiling. On the other hand, in extra-SC the main impairment would come from the strong sunlight, hence the DLOS architecture has to be preferred, thanks to much higher robustness to the background light [30].

The TX involves an optical source emitting at $850\,\mathrm{nm}$, close to the responsivity peak of the silicon-based PDs. Moreover, this choice of wavelength is convenient to reject the ambient light noise in the visible region, i.e. sunlight in extra-SC and artificial light in AIT.

In the NLOS links, the light source is a Light Emitting Diode (LED), which has a wider emission angle and a higher optical power than the laser diode. The designed TX driver is an electronic circuit that converts the single-ended $0\,\mathrm{V}$ to $5\,\mathrm{V}$ signal into a current signal that directly drives the optical source. Our driver is based on a high-speed and high-current rugged RF power transistor, which is designed for communication and aerospace application. It has been optimized for the OOK transmission at 2 Mbit/s.

For the DLOS architecture, a Vertical Cavity Surface Emitting Laser (VCSEL) is the most suitable source: it has a low power consumption and a quite narrow emission angle, thus minimizing the required power. Moreover, a VCSEL has also a narrow optical bandwidth ($\sim 1\,\mathrm{nm}$), which allows for a very narrow and effective optical filtering at RX, which is very useful in the extra-SC scenario to remove the sunlight. In this case, the driver is slightly different, as the VCSEL requires a quite lower electrical current.

C. Receiver Board

The RX module is made of the PD and a cascade of three electrical amplifiers: the Transimpedance Amplifier (TIA), a Voltage Gain Amplifier (VGA), and a comparator.

In all cases the sensor is a PIN-PD, thus minimizing the size, the cost and the power consumption. We selected the same optical sensor for both versions of the transceiver: it has an active area of $25\,\mathrm{mm}^2$ with a responsitivity of $0.55\,\mathrm{A/W}$ at $850\,\mathrm{nm}$. The only difference is that, in the DLOS version, the sensor is molded with a plastic lens ($14\,\mathrm{mm}$ diameter, $9.8\,\mathrm{mm}$ focal

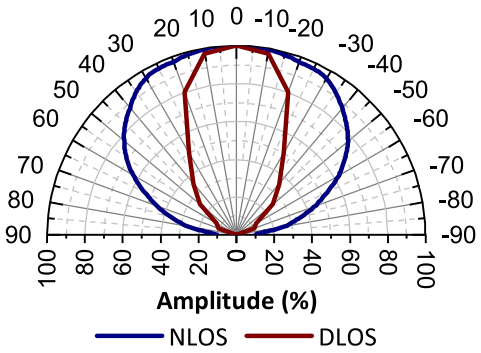

Fig. 5. Directivity diagram of the two optical detectors (NLOS and DLOS) used in the proposed RXs.

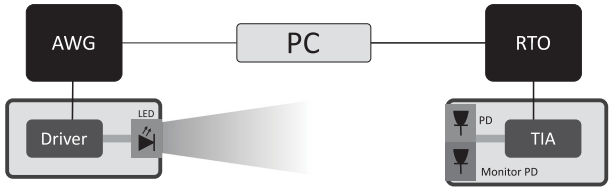

Fig. 6. Experimental setup for the NRZ transmission; AWG: Arbitrary Waveform Generator; PD: Photo-Diode; RTO: Real-Time Oscilloscope; TIA: Transimpedance Amplifier.

length), reducing the FOV and increasing the effective active area of the RX to $150\,\mathrm{mm}^2$. The directivity of the two RXs are reported in Fig. 5; here, we see that the FOV reduces from $\pm 65^\circ$ to $\pm 30^\circ$. The optical sensor has a significant responsivity only in the $700\,\mathrm{nm}$ to $1100\,\mathrm{nm}$ range, strongly reducing the impact of the visible light components.

Since we always use the same PIN-PD device, also the other parts of the electronic board are the same, strongly reducing the complexity and increasing the flexibility of the solution. The transimpedance circuitry is AC-coupled to reject the ambient light and to avoid the saturation of the amplifiers due to any strong ambient light. Its output data have a voltage amplitude ($0\,\mathrm{V}$ to $5\,\mathrm{V}$) suitable to be fed back to the signal adapter (*IN* port in Fig. 3). The VGA provides an optimized amplification gain from -20+20 dB, which can be externally controlled. The comparator has a fixed input threshold that allows to restore an OOK output signal with the proper voltage.

IV. Experimental Results

A. NRZ Characterization

We first characterized the TX and the RX modules, using a NRZ signal. We measured the eye diagram and the Bit Error Ratio (BER) as a function of the average received optical power P.

These measurements were performed using the experimental setup reported in Fig. 6. Since no current Pseudo-Random Binary Sequence (PRBS) equipment can work at the considered bit rate, we generated a 2 Mbit/s PRBS NRZ sequence of $1 \times 10^8\,\mathrm{bits}$ by an Arbitrary Waveform Generator (AWG), driven by a Matlab script running on a PC. We selected 2 Mbit/s

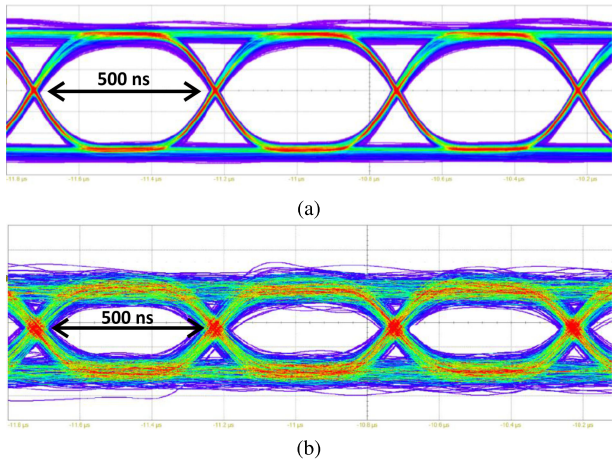

Fig. 7. Eye diagrams of the NRZ transmission taken at -30 dBm (a) and at -40 dBm (b). Vertical scale is 50mV/div (a) and 12mV/div (b).

to emulate closely the spectral features of the Manchester signal of the MIL-STD-1553B. The AWG output was used to directly drive the optical source (peak optical power of 30 dBm and 0 dBm for NLOS and DLOS transceiver, respectively) by means of the TX driver, described in Section III-B. After free-space transmission, the RX output was recorded by a Real-Time Oscilloscope (RTO) set a $250\,\mathrm{MSa/s}$ and acquired by the same PC for the BER measurement, based on a home-made routine. To simulate different levels of received intensity, we placed a variable optical attenuator in front of the TX; this can add variable losses without changing the optical properties of the signal.

At the RX side, very close to the PD, we placed a DC-coupled monitoring PD, which measures P. P can be also measured from the amplitude of the TIA output, knowing the gain and the responsivity of our PD.

We report in Fig. 7 the eye diagrams of the received signal after the TIA, taken with a clock signal at $2\,\mathrm{MHz}$, at $P = -30\,dBm$ and $P = -40\,dBm$, respectively.

As can be seen, in both cases the RX produces open eye diagrams. Indeed, we did not observe any error after the transmission. We note that, for our application, we should know the sensitivity, i.e. the received optical power, at BER $= 1 \times 10^{-12}$. However, in our case the minimum measurable BER is very limited. A basic calculation shows that a BER $< 1 \times 10^{-12}$ requires at least 5 days for a real-time measurement, this would by far increase here since we must use offline processing. Therefore, a direct measurement of this sensitivity is unfeasible.

However, we can extrapolate the BER information by referring to the theory: since our performance is only affected by the RX noise, the BER curve has a linear trend if reported in double-log Y-scale as a function of the received optical power (in dBm) [31]. Extending the linear fit down to the level of BER $= 1 \times 10^{-12}$ allows us to estimate the required received optical power for the target BER.

The resulting BER curves for the two RXs are reported in Fig. 8. The sensitivities (at BER $= 1 \times 10^{-12}$) are -41 dBm

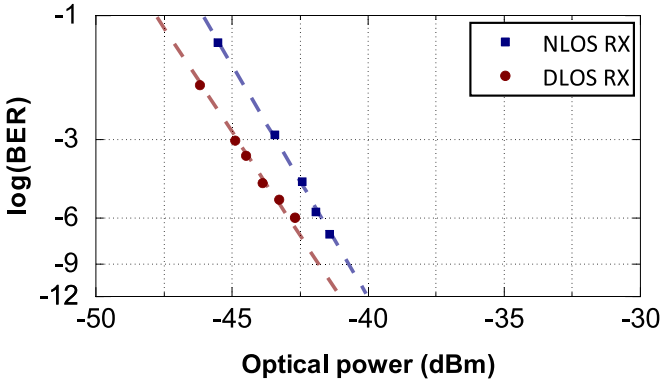

Fig. 8. RX sensitivity measurement with a NRZ signal.

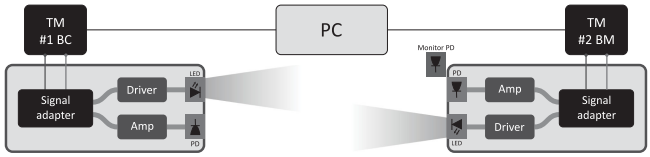

Fig. 9. Experimental setup for MIL-STD-1553B performance test. TM: Test Module.

and −40 dBm for DLOS and NLOS receivers, respectively. Although the two RXs are very similar, the actual sensitivity is slightly different (∼1 dB): this is likely due to a slightly different gain on the two TIAs.

For simplicity, we reported the BER curves as function of the total received power. However, in a real scenario, we should better consider the optical power density at the receiver: in that case, the effect of the lens would be clear, because it increases the power received by the PD by around 8 dB.

In both cases, the sensitivity is below −40 dBm, i.e. the expected sensitivity for a PIN PD for 2 Mbit/s NRZ transmission. This demonstrates that the front-end of the RXs complies with the expected value, as can be derived by the PD specification.

B. MIL-STD-1553 Sensitivity Measurement

For the complete characterization, we then performed MIL-STD-1553B transmission experiments. Transmitting MIL-STD-1553B is fairly different than transmitting pure NRZ signals (see Section II). Therefore, we had to develop a custom setup for the laboratory characterization of the MIL-STD-1553B bus with the TOWS transceiver, which we present in Fig. 9.

The signal was generated by means of a Test Module (TM) by Avionics Interface Technologies, compliant with the MIL-STD-1553B standard. These TMs allow to simulate the bus MIL-STD-1553B and the correct interactions among the devices of the bus: BC, RTs and BM. Furthermore, these TMs can perform a vary detailed signal analysis, since they are provided with a driver software to develop custom C# application interfaces. Thanks to this feature, we realized up a home-made routine for transmission and detection of MIL-STD-1553B signal, which generates and acquires the different words in hexadecimal format and converts them in a binary stream for BER analysis.

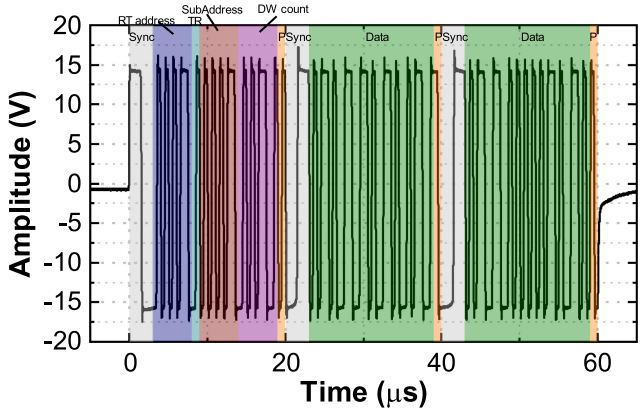

Fig. 10. Benchmark signal from BC to RT used to characterize the transceiver. We can identify a CW and two DWs for a total of 60 μs.

For the experimental characterization of the TOWS transceiver, we simulated a link between a BC and a RT (address 1, sub-address 1). We stick strictly to recommendations of the MIL-STD-1553B standard hence, the benchmark signal was composed by a CW and two DWs (`35b2 281b`, in hexadecimal format) and it is reported in Fig. 10. The choice of RT addresses and of DWs number it is not relevant to the RX characterization.

The electrical waveform was generated by the first TM (TM#1, working as BC) and fed to the signal adapter board. This board generates the waveform for the optical source TX and also generates the rectangular pulse of a time window needed to disable the back-reflected signal (*DIS* in Fig. 4). After free-space transmission, the optical signal was detected by the RX belonging to another identical transceiver placed at $1.5\,\mathrm{m}$ from the TX. The electrical signal was then converted back into a differential waveform and detected by the second TM (TM#2, working as RT/BM). Eventually, the received signal was extracted and analyzed by a routine running on the PC connected to TM#2. The routine compares the transmitted and received sequences of bits and then computes the BER value; from a set of BER values measured at different power levels, we estimated the sensitivity. We recall that MIL-STD-1553B standard requires a BER lower than 1×10^{-12} [19]. As for the NRZ characterization, the BER was measured transmitting 1×10^8 bits (around $45\,\mathrm{min}$).

In Fig. 11, we report the results taken at two different values of the optical power (-30 dBm and −40 dBm) at the output of the TIA, with a $2\,\mathrm{MHz}$ clock: in this condition, the eye diagram is similar to that of a typical NRZ signal at 2 Mbit/s, as we can see in Fig. 12. This signal is converted back to bipolar Manchester-encoded by the subsequent electrical adaptation, as we show in Fig. 13 where the upper part is the input unipolar signal and the lower part is the output bipolar signal.

Varying P at the receiver in a range between −37 dBm and −43 dBm, we obtained the BER curve that is shown in Fig. 14. As expected, the measured values well fit a straight line, once the BER is in double-log scale. From this curve, we can estimate the RX sensitivity, by extrapolation; here we find that the average P value of −37.5 dBm corresponds to BER $= 1 \times 10^{-12}$. This

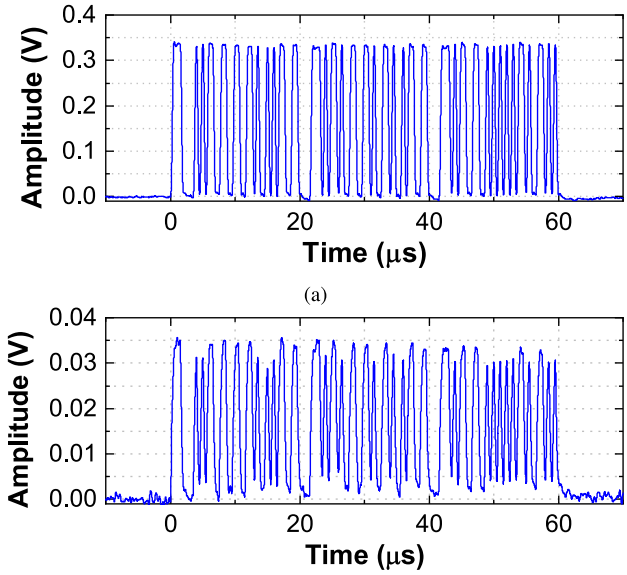

(a)

(b)

Fig. 11. Received unipolar waveforms at TIA output, taken at -30 dBm (a) and at -40 dBm (b).

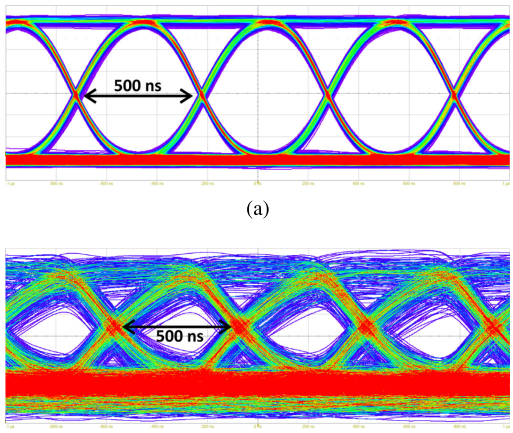

(a)

(b)

Fig. 12. Received eye diagrams at TIA output, taken with a $2\,\mathrm{MHz}$ clock, at -30 dBm (a) and at -40 dBm (b). Vertical scale is $50\,\mathrm{mV/div}$ (a) and $12\,\mathrm{mV/div}$ (b).

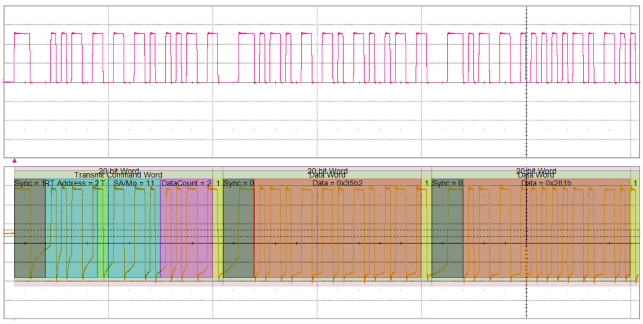

Fig. 13. Detection of MIL-STD-1553B signal after OWC transmission. We show the traces of the detected signal after the comparator (top) and of the reconstructed differential signal ($A - B$) (bottom). The last also includes the MIL-STD-1553B decoding performed by the RTO.

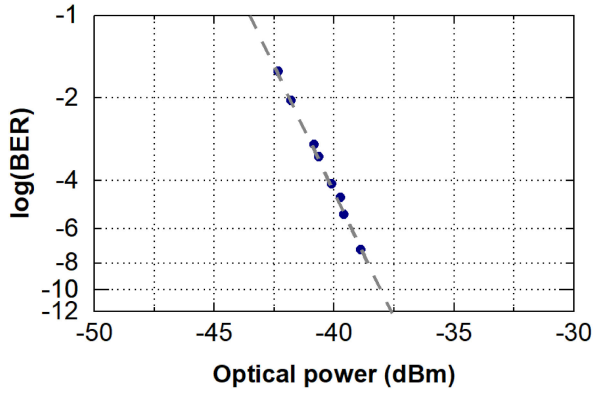

Fig. 14. BER measurements for MIL-STD-1553B signal, taken as a function of the received optical power.

gives an overall power budget of around $+65\,dB$, considering an average transmitter power of 27 dBm.

We see that this RX sensitivity is slightly worse (by around $2.5\,dB$) than the NRZ sensitivity from Fig. 8. This penalty is due to the difference on the data recovery algorithm used in the two cases: when using NRZ signals, the offline processing automatically adapts the threshold for data recovery every $500\,\mu\mathrm{s}$; on the other hand, when using the MIL-STD-1553B signal, the threshold of the RX comparator is fixed during all the BER measurements. Therefore, any low-frequency noise captured by the RX affects the BER. We expect that, with an optimized PCB design and exploiting a dynamically-optimized threshold, this penalty can disappear.

We highlight that we choose a transmission distance to be consistent with a satellite dimension and with intra-SC transmission. However, since the sensitivity measurements allow to establish a general system parameter, they do not depend on the transmission distance or the transceiver position and orientation.

V. Conclusion

We designed and realized an innovative implementation of a OWC system that can be used to interface the MIL-STD-1553B terminals, thus replacing the cables in various SC applications. To this aim, the transceivers implement a transparent solution, which is completely analog. This guarantees full compatibility with the existing electronics and therefore we need no modification of the protocols and of the bus architecture. This approach leads to a flexible implementation of the transceiver: all the key elements of TX and RX remain the same in the different application scenarios (intra, extra or AIT), whereas the optimization is obtained by means of minor modifications.

First, the OWC section of the transceivers was experimentally characterized by means of eye diagrams and sensitivity measurements, using common NRZ signals. It was then successfully interfaced with MIL-STD-1553B signals, generated by commercial test units. The obtained results clearly demonstrate the potential of the proposed solution as well as the complete compatibility with the MIL-STD-1553B transmission boards.

This makes the proposed approach highly promising for the expected application scenarios.

The proposed transceivers are made of commercially available devices, they have small size and low power consumption, both of which could be further improved. These features make them very attractive for the deployment, also considering that all the current components can be replaced by similar devices that are space-graded.

We also note that, although the primary application for the presented development is in the space industry, these MIL-STD-1553B-OWC interfaces could easily be deployed in other environments, e.g. on airplanes.

Finally, we note that this first implementation was focused on the MIL-STD-1553B standard, but we are confident that our approach can be extended to transport also other protocols over optical wireless signals.

REFERENCES

[1] T. Ricker, "Avionics bus technology: Which bus should i get on," in *Proc. IEEE/AIAA 36th Digit. Avionics Syst. Conf.*, 2017, pp. 1–12.

[2] P. Fortescue, G. Swinerd, and J. Stark, *Spacecraft Systems Engineering*. New York, NY, USA: Wiley, 2011.

[3] R. Krishnan and V. R. Lalithambika, "A comparison of AFDX and 1553B protocols using formal verification," in *Proc. Int. Conf. Adv. Comput., Commun. Inform.*, 2018, pp. 1617–1623.

[4] R. Amini *et al.*, "New generations of spacecraft data handling systems: Less harness, more reliability," in *Proc 57th Int. Astronautical Congr.*, 2006, pp. D1–D4.

[5] D. R. Dhatchayeny, S. Arya, and Y. H. Chung, "Infrared-based multiple-patient monitoring in indoor optical wireless healthcare systems," *IEEE Sensors J.*, vol. 19, no. 14, pp. 5594–5599, Jul. 2019.

[6] M. Uysal *et al.*, *Optical Wireless Communications: An Emerging Technology, Ser. Signals and Communication Technology*. Berlin, Germany: Springer International Publishing, 2016.

[7] Z. Sun *et al.*, "Wireless RF bus design for an intra-satellite," *J. Harbin Eng. Univ.*, vol. 33, no. 7, pp. 881–886, 2012.

[8] "Wireless network communications overview for space mission operations," Consultative Committee for Space Data Systems, Informational Rep. CCSDS 880.0-G-3, Green Book, pp. 42–47, May 2017.

[9] N. Karafolas, J. M. P. Armengol, and I. Mckenzie, "Introducing photonics in spacecraft engineering: Esa's strategic approach," in *Proc. IEEE Aerosp. Conf.*, 2009, pp. 1–15.

[10] A. Grindle, O. de Weck, and S. Shull, "An autonomous, real-time asset management system for the international space station: Net present value analysis," in *Proc. Amer. Inst. Aeronaut. Astronaut. SPACE Conf. Expo.*, 2008, pp. 7607–7625.

[11] S. Das, S. S. Das, and I. Chakrabarti, "Hardware implementation of MIL-STD-1553 protocol over OFDMA-PHY based wireless high data rate avionics systems," in *Proc. IEEE Int. Conf. Adv. Netw. Telecommun. Syst.*, 2016, pp. 1–6.

[12] R. Onrubia *et al.*, "Satellite cross-talk impact analysis in airborne interferometric global navigation satellite system-reflectometry with the microwave interferometric reflectometer," *Remote Sens.*, vol. 11, no. 9, pp. 1120–1130, 2019.

[13] H. Zhou, M. Jong, and G. Lo, "Evolution of satellite communication antennas on mobile ground terminals," *Int. J. Antennas Propag.*, vol. 2015, pp. 282–295, Oct. 2015.

[14] N. Karafolas *et al.*, "Optical communications in space," in *Proc. Int. Conf. Opt. Netw. Des. Model.*, 2009, pp. 1–6.

[15] H. Guerrero *et al.*, "Optical wireless links for intra-satellite communications (OWLS): The merger of optoelectronic and micro/nano-technologies," in *Proc. NanoTech 2002- At the Edge of Revolution*, 2002, pp. 5754–5765.

[16] A. Santamaria *et al.*, "Wireless infra-red links for intra-satellite communications," in *Proc. -Data Syst. Aerosp.*, 2003, vol. 532, pp. 49.1–49.6.

[17] S. Rodriguez *et al.*, "Optical wireless MIL-STD-1553 and serial synchronous buses for intra-spacecraft communications," in *Proc. Data Syst. Aerosp.*, vol. 602, pp. 22.1–22.12, 2005.

[18] H. Guerrero, "Optical wireless intra-spacecraft communications," in *Proc. Eur. Space Agency Special Pub.*, 2006, vol. 621, pp. 177.1–177.6.

[19] MIL-STD, "1553B: Digital time division command/response multiplex data bus," Department of Defense, 1978.

[20] I. Arruego *et al.*, "OWLS: A ten-year history in optical wireless links for intra-satellite communications," *IEEE J. Sel. Areas Commun.*, vol. 27, no. 9, pp. 1599–1611, Dec. 2009.

[21] L. Zhou and J. An, "Research on wireless MIL-STD-1553B bus based on infrared technology," *J. Netw.*, vol. 9, pp. 2690–2696, 2014.

[22] S. Das, N. Chandrakar, and S. S. Das, "MIL-STD-1553 based wireless visible light communication system," in *Proc. IEEE Int. Conf. Adv. Netw. Telecommun. Syst.*, 2016, pp. 1–6.

[23] M. Z. Chowdhury, M. K. Hasan, M. Shahjalal, M. T. Hossan, and Y. M. Jang, "Optical wireless hybrid networks: Trends, opportunities, challenges, and research directions," *IEEE Commun. Surv. Tut.*, vol. 22, no. 2, pp. 930–966, Apr.–Jun. 2020.

[24] A. Al-Kinani, C. -X. Wang, L. Zhou, and W. Zhang, "Optical wireless communication channel measurements and models," *IEEE Commun. Surv. Tut.*, vol. 20, no. 3, pp. 1939–1962, Jul.–Sep. 2018.

[25] G. Cossu, R. Corsini, and E. Ciaramella, "High-speed bi-directional optical wireless system in non-directed line-of-sight configuration," *J. Lightw. Technol.*, vol. 32, no. 10, pp. 2035–2040, 2014.

[26] S. Arnon *et al.*, *Advanced Optical Wireless Communication Systems*. New York, NY, USA: Cambridge Univ. Press, 2012.

[27] H. Kaushal and G. Kaddoum, "Optical communication in space: Challenges and mitigation techniques," *IEEE Commun. Surv. Tut.*, vol. 19, no. 1, pp. 57–96, Jan.–Mar. 2017.

[28] E. Ciaramella *et al.*, "TOWS: Introducing optical wireless for satellites," in *Proc. 21st Int. Conf. Transparent Opt. Netw.*, 2019, pp. 1–4.

[29] Maxim Integrated, "RS-485 Transceiver with integrated low-dropout regulator and autodirection control," Aug. 2009, [Online]. Available: https://datasheets.maximintegrated.com/en/ds/MAX13410E-MAX13413E.pdf

[30] Z. Ghassemlooy, W. Popoola, and S. Rajbhandari, *Optical Wireless Communications: System and Channel Modelling With MATLAB*, 2nd ed. Boca Raton, FL, USA: CRC Press, 2019.

[31] G. Agrawal, *Fiber-Optic Communication Systems, Ser. Microwave and Optical Engineering*. New York, NY, USA: Wiley, 2012.